Reconfigurable Thermoelectric Generators for Vehicle Radiators Energy Harvesting

Donkyu Baek*, Caiwen Ding†, Sheng Lin†, Donghwa Shin‡, Jaemin Kim§,
Xue Lin¶, Yanzhi Wang†, and Naehyuck Chang*
* Korea Advanced Institute of Science and Technology, Korea, † Syracuse University, USA, ‡ Yeungnam University, Korea,
§ Seoul National University, Korea, ¶ Northeastern University, USA
*{donkyu,naehyuck}@cad4x.kaist.ac.kr, †{cading,shlin,ywang393}@syr.edu, ‡donghwashin@yu.ac.kr,
§jmkim@elpl.snu.ac.kr, and ¶xuelin@coe.neu.edu

***Abstract*—Conventional internal combustion engine vehicles (ICEV) generally have less than a 30% of fuel efficiency, and the most wasted energy is dissipated in the form of heat energy. The heat energy maintains the engine temperature for efficient combustion as a good aspect, but the amount of heat generation is excessive and eventually breaks the engine components unless advanced cooling system technologies are supported such as high-capacity radiators, elaborated water jackets, high-flow rate coolant pumps, etc. The excessive heat dissipation plays a key role on a poor fuel economy, but reclamation of the heat energy has not been a main focus of vehicle design.**

This work is first to propose a cross-layer, system-level solution to enhance thermoelectric generator (TEG) array efficiency introducing online reconfiguration of TEG modules. The proposed method is useful to any sort of TEG array to reclaim wasted heat energy because cooling and exhaust systems generally have different inlet and outlet temperatures. In this paper, we deploy the proposed method to vehicle radiator heat energy harvesting, which does not affect the vehicle performance while exhaust heat energy harvesting may disturb the combustion and emission control integrity. We introduce a novel TEG reconfiguration and maximize the TEG array output in spite of dynamic change of the coolant flow rate and temperature, which results in a huge variation in the coolant temperature distribution of inside the radiator. The proposed method enables all the TEG modules to run at or close to their maximum power points (MPP) under dynamically changing vehicle operating conditions. Experimental results show up to a 34% enhancement compared with a fixed array structure, which is a common practice.

I. Introduction

The cooling system is one of the most essential components in internal combustion engine vehicles (ICEV) that makes it possible to achieve small but powerful engines allowing continuous and long-lasting operations. The excessive heat generation from the engine is theoretically explained by Carnot Limit, and approximately 1/3 of the fuel consumption is wasted in the form of heat. About a half of the generated heat goes through the engine cooling system, which leads to additional energy consumption for releasing the heat [1].

Modern ICEV is equipped with water cooling systems. Coolant flows through the water jacket in the engine block and cylinder head and cools down the engine components such as valves, cylinder block, etc. The hot coolant is cooled down in the radiator, a heat exchanger. The radiator dissipates heat with natural convection while the vehicle is moving, but forced-convection air cooling is often required under many circumstances, which consumes additional energy. Coolant flow is generated by a coolant pump, which also consumes significant energy. Radiator fans and cooling pumps can be driven either by the engine crank shaft or the vehicle battery, which is again charged by the alternator driven by the engine crank shaft. Therefore, higher cooling capacity consumes more fuel energy for cooling.

978-1-5090-6023-8/17/$31.00

Many previous practices on cooling control and optimization methods have been conducted to investigate the state-of-the-art vehicle radiators in order to minimize power consumption [2]. A mathematical model of radiator fans and a forced-convection heat transfer process have been developed to establish a mixed integer nonlinear programming problem, and an interior points approach has been developed to solve the minimization problem in [3]. The emergence of computer-aided design (CAD) software and finite element methods (FEM) are changing the modeling of automotive radiators and analysis of their structural behavior [4]. In this paper, we borrow a radiator model from [5].

There are many ways to convert heat energy to other forms of energy. Converting the heat energy to electric energy is desirable because the electric energy can be easily stored and converted to other forms of energy. A thermoelectric generator (TEG) is a device that directly converts heat energy to electric energy by the Seebeck effect. It is a solid device without a moving part and thus is easy to handle.

A large portion of vehicle heat energy harvesting has been attempted from exhaust pipes. Exhaust pipes carry very hot combusted gas so that an efficient medium-temperature TEG can be applied, and it is reported that a few hundreds Watts of power can be harvested from a light-duty vehicle [6], [7]. However, there are obvious downsides in the exhaust heat energy harvesting because TEG installation in the hot exhaust pipes around the catalyst may significantly affect the emission control integrity and engine power. To avoid such side effects, TEG modules are often installed after the catalyst where the exhaust gas is already cooled down significantly. In addition, the exhaust pipe surface is much cooler than the exhaust gas itself. Therefore, there have been many attempts to install TEG modules inside the exhaust pipe. However, such a method may alter the engine back pressure, and cooling the TEG cool side becomes challenging. The TEG modules are vulnerable to be damaged due to severe vibration as well.

Typical coolant inlet temperature is not higher than 100°C, and low temperature TEG modules can be integrated with the cooling system. Low temperature TEG modules integrated with a a light-duty vehicle radiator were reported to harvest around 75 W [8]. In spite of such a low energy density from radiator energy harvesting, there are also obvious advantages. Low temperature TEG modules are much more affordable than medium-to-high temperature ones. However, we do not emphasize the pros and cons of the radiator energy harvesting over the exhaust energy harvesting in this paper. We focus on the system level solution to leverage the TEG module

efficiency. Most of all, the proposed method is very useful both for exhaust and radiator energy harvesting, moreover, the proposed method can be applied to any kinds of wasted heat energy harvesting including factory facility environment.

Multiple TEG devices generally form a module to generate a usable voltage level. In addition, a large number of TEG modules, typically connected in series and parallel, ensure the required power and energy densities. However, even with a large number of TEG modules, it is natural to use a single power converter connected to the both ends of the series-parallel TEG module array.

Large number of TEG modules occupy a significant surface area. Any cooling or exhaust system, which carries coolant or gas, gradually loses heat energy and temperature toward the outlet. A part of TEG modules is located next to the inlet while some others are located nearby the outlet. Therefore, each TEG module must have different hot side temperatures; TEG modules close to the inlet have a higher hot side temperature and vice versa. We focus on one of the most challenging problems such that all the TEG modules should operate at their maximum power point (MPP) even if they have different hot side temperatures but are connected all together in series and parallel.

We perform real measurement of a production ICEV and confirm that the coolant temperature in the radiator significantly decreases from the inlet to outlet, and the temperature difference is up to 60° C even in summer, and the temperature distribution dynamically changes by the driving condition. This explains that none of the TEG modules attached to the radiator has the same hot side temperature, and their hot side temperatures vary all the time. Therefore, a fixed series and parallel connection of TEG modules cannot ensure the MPP operation of the TEG modules even though the charger has the MPPT (maximum power point tracking) capability.

In this paper, we introduce the radiator temperature measurement, modeling and simulation. This paper shows the experimental setup to characterize the real coolant behavior and performance evaluation of the proposed methods under the real vehicle driving condition. Our problem formulation describes the optimal TEG module reconfiguration to achieve the MPP operation under dynamically changing coolant temperature and flow rate. We devise algorithms with a polynomial time complexity to find the best TEG module array configuration for a given coolant flow rate, inlet temperature, airflow (vehicle speed), and ambient temperature.

Conventional methods cannot optimize the number of series-parallel connections for dynamically changing coolant inlet temperature and flow rate, which largely vary by the vehicle driving conditions. Experimental results exhibit up to a 34% performance enhancement compared with a 10 by 10 fixed array TEG modules.

II. Component Models

A. Radiator Model

We employ a radiator model as a finned-tube heat exchanger (coolant in tubes, air in cross flow) from [5]. This model is constructed under the following assumptions: (i) the dissipated heat only travels through the radiator; (ii) the coolant flow rate in the coolant tube is uniformly distributed through the radiator, and the coolant is in a fully flowing condition in the tube; and (iii) both fluids (coolant and ambient air) are considered as incompressible flow and unmixed at any intersection between paths.

We adopt the NTU (number of heat transfer units) method to determine the effectiveness of the radiator as a heat exchanger [5]. This method involves three dimensionless parameters to be calculated including NTU, effectiveness (i.e., ε) and heat capacity ratio (i.e., C_r). The heat capacity ratio is defined as

$$C_r = C_{min}/C_{max} \tag{1}$$

where C_{min} equals to the minimal one between C_a and C_c, and C_{max} equals to the maximal one between C_a and C_c. C_a and C_c stand for the heat capacity rate for the ambient air and the coolant, respectively. They are calculated by

$$C_a = m_a \times c_{p,a} \text{ and } C_c = m_c \times c_{p,c} \tag{2}$$

where m_a and m_c are the flow rates of ambient air and coolant, respectively, and $c_{p,a}$ and $c_{p,c}$ are the specific heat capacities of the ambient air and coolant, respectively. NTU is widely used for heat exchanger analysis and is defined as

$$NTU = \frac{U \times A}{C_{min}} \tag{3}$$

where U denotes heat transfer coefficient, and A represents the radiator surface area. The heat exchanger effectiveness ε is obtained by

$$\varepsilon = 1 - e^{(\frac{1}{C_r} \times NTU^{0.22} \times (e^{(-C_r \times NTU^{0.78})} - 1)}. \tag{4}$$

The maximum possible heat transfer rate i.e., Q_{max} for the exchanger is defined as

$$Q_{max} = C_{min} \times (T_{c,in} - T_{a,in}) \tag{5}$$

where $T_{c,in}$ and $T_{a,in}$ denote the inlet temperatures of the coolant and ambient air, respectively. The actual heat transfer rate is determined from the expression

$$Q = \varepsilon \times Q_{max}. \tag{6}$$

The coolant and ambient outlet temperatures are

$$T_{c,out} = T_{c,in} - Q/C_c \text{ and } T_{a,out} = T_{a,in} + Q/C_a. \tag{7}$$

The temperature profile along the radiator fins is obtained by

$$T_{pf} = (T_{c,in} - \frac{T_{a,out} + T_{a,in}}{2}) \times e^{\frac{-U}{C_c} \cdot A_{var}} + \frac{(T_{a,out} + T_{a,in})}{2} \tag{8}$$

where A_{var} is the area vector for local temperature derivation, and therefore T_{pf} is a vector with the same dimension as A_{var}.

B. Model and Characterization of a TEG module

A TEG device comprises of a top, a bottom ceramic plates (thermoelectric materials) and internal pellets. A group of TEG devices is packaged together and forms a module. The bottom ceramic plate attaches to the hot side. In this particular application, this side faces with the radiator surface. A heatsink, i.e, a radiator pin, attaches to the top ceramic and exposes into the ambient air, which forms the cool side. The actual installation of the TEG modules requires modification of the radiator. TEG modules reside between the radiator surface and radiator fins while the factory radiators have integrated structure of the radiator surface and fins.

The TEG module generates electrical energy from the temperature difference between the bottom and top ceramic plates. We assume that the heatsink and ambient air have the same temperature; the ambient airflow is enough to fast, which is a typical operating condition of vehicle radiators.

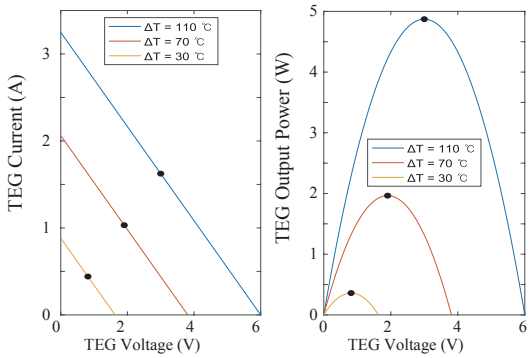

Fig. 1. The derived (a) V-I (b) V-P output characteristics of the selected TEG module by temperature (TGM- 199-1.4-0.8) [9].

The output power of the TEG module is estimated by the following formulas:

$$E_{teg} = \alpha \times (T_{pf}[i] - T_{amb}) \times N_{cpl}, \tag{9}$$

$$I_{teg} = \frac{E_{teg}}{R_{teg} + R_{load}}, \tag{10}$$

$$P_{teg} = I_{teg}^2 \times R_{load} \tag{11}$$

where α is the Seebeck coefficient, $T_{pf}[i]$ is the local radiator fins temperature where TEG module is attached, T_{amb} is the temperature of ambient air, N_{cpl} is the number of the couples, and R_{teg} and R_{load} stand for the TEG module resistance and load resistance, respectively.

We extract the voltage-current (V-I) and voltage-power (V-P) output characteristics of the TEG module used in this work (TGM-199-1.4-0.8) under different ΔT where $\Delta T = T_{pf}[i] - T_{amb}$. The black dots in Fig. 1 (a) and (b) are their maximum power points (MPP.)

III. Problem Formulation

A. A TEG Module Array on Radiator

We assume an 1-dimensional radiator structure in this paper for easy delivery of the most important technical contributions. The real vehicle radiators have a 2-dimensional structure, which can be explained with multiple parallel connections of the 1-dimensional radiator. There are also temperature differences at fork, each inlet of the parallelly connected 1-dimensional radiators. We leave the model expansion to a 2-dimensional radiator model for future work in this paper.

Fig. 2 illustrates an S-shaped 1-dimensional pipe structure radiator with TEG module arrays. There are N TEG modules attached on the radiator where $T_{pf}[i]$ is the radiator surface temperature at the location of TEG i ($1 \leq$ i $\leq$ N) obtained from (8). Therefore, the temperature difference between the bottom and top ceramic of TEG i is $\Delta T_i = T_{pf}[i] - T_{amb}$.

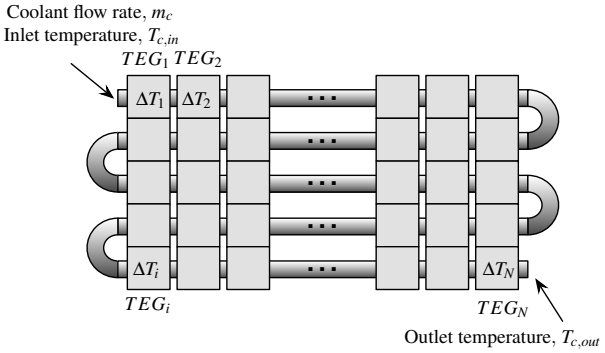

Fig. 2. A TEG module array attached to the 1-dimensional S-shaped radiator.

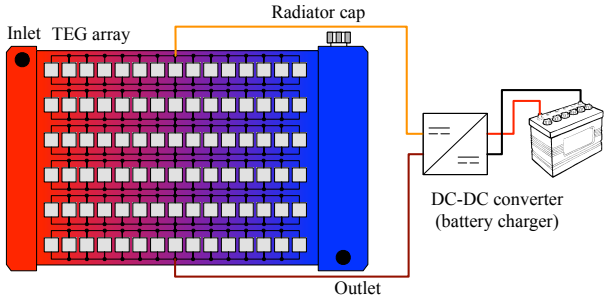

Fig. 3. A fixed regular array, a series-parallel, connected TEG module array on a radiator: the baseline setup (a common practice.)

Once again, along the radiator pipe from the coolant inlet to the outlet, $T_{pf}[i]$ and also ΔT_i gradually decrease, which is the key motivation of this work. Each TEG module has a different coolant temperature (their hot side temperature) as the coolant is gradually but significantly cooled down while their cool side temperature is the same, i.e., each ΔT_i is not the same. This results in different MPP voltage and current values by TEG modules.

Previous work [10] commonly assumed that the array of TEG modules has fixed series-parallel electrical connections where each row of the array has the same number of TEG modules as shown in Fig. 3. Ideally, the TEG module array can achieve output power as high as the sum of the MPP power of each TEG module if all the TEG modules operate at their MPP. Unfortunately, none of TEG modules in Fig. 3 is guaranteed to operate at their MPP even if the endpoint charger has the MPPT feature. As a result, the entire TEG module array poorly produces electrical energy. We are first to point out this issue for wasted heat energy harvesting with TEG modules, which is the first technical contribution of this work. Moreover, we fix this problem with a system-level solution, which is the main technical contribution of this paper.

Fig. 4 visualizes the reason for TEG module power loss caused by temperature differences [10]. The MPP line is denoted in green while the actual operating points are illustrated in red. This is because all the TEG modules must have the same output voltage when they are connected in parallel as shown in Fig. 4 (a), and all the parallelly connected TEG module groups must have share the same amount of current when they form a series string as shown in Fig. 4 (b). Comparing with the sum of power values in blue dots, the total power generation from the TEG array, i.e., the sum of power values in red dots, is extremely poor. A brute-force cure to solve this problem is to connect an individual power converter

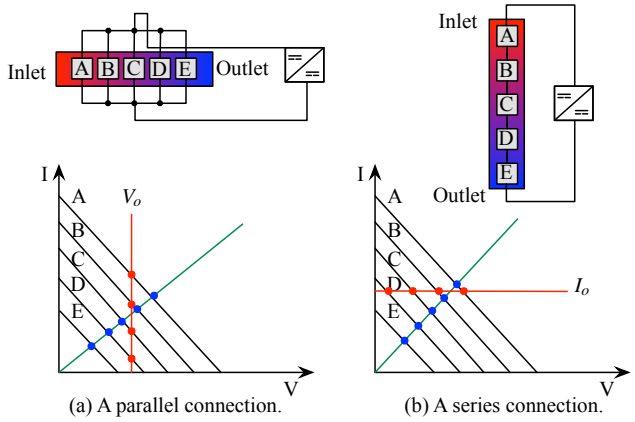

Fig. 4. TEG module output power loss due to the differences in the hot side temperatures among the connected modules.

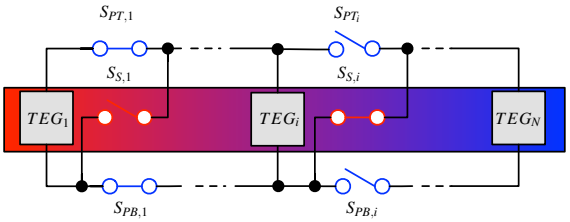

Fig. 5. Architecture of the proposed reconfigurable TEG module array.

to each TEG module, aka., a micro-converter architecture. Such a method provides the maximum power output despite the hot side temperature differences with a great expense of cost, which the real automotive market cannot afford.

B. TEG Array Reconfiguration

We propose a system-level solution to overcome the output power loss [1] of TEG module array caused by spatial temperature variation in the radiator. We borrow the reconfigurable switch network, which was introduced for the photovoltaic systems [11]. TEG reconfiguration has been mentioned in [12], but this work tries to change between all in series and all in parallel. In addition, they assume that all the TEG modules have the same temperature difference to obtain better power converter efficiency. Also, the number of switches are more than those in [11].

Fig. 5 illustrates the electrical connections of the reconfigurable array of N TEG modules. Each TEG module (except for the N-th one) is integrated with three solid-state switches: a top parallel switch $S_{PT,i}$, a bottom parallel switch $S_{PB,i}$ and a series switch $S_{S,i}$. The parallel switches connect TEG modules in parallel while the series switches connect TEG modules in series. We reconfigure the array dimension (i.e., electrical connections) of the TEG modules by controlling the ON/OFF states of the switches without changing their physical location. Most importantly, the switch network configures imbalanced array structures where each row has a different number of columns. This is the key feature to enable the use of a single power converter while maintaining the near MPP of all the TEG modules with largely different hot side temperature values among TEG modules.

Fig. 5 shows the configuration to make a series or parallel connection by the use of two series switches and a parallel switch. The TEG_1 is connected in parallel to TEG_2 as both the parallel switches on top and bottom are ON leaving the series switch OFF. On the other hand, TEG_{N-1} is connected to TEG_N in series.

We provide a formal description of the TEG module array configuration. Let us consider a reconfigurable TEG module array with N TEG modules. It may have an arbitrary number of TEG module groups, i.e., g ($\leq N$). There are r_j parallelly connected TEG modules in the j-th TEG module groups:

$$\sum_{j=1}^{g} r_j \leq N. \tag{12}$$

Fig. 6 illustrates the system configuration of a vehicle radiator heat energy harvesting that includes the proposed reconfigurable TEG module array. The key subsystems include a reconfigurable TEG module array, a battery charger, a vehicle battery, and a reconfiguration controller. Typical lead-acid car battery charging voltage is 13.8 V, and we optimize the reconfiguration to 13.8 V. The TEG module array is connected to the battery charger that is cable of the MPPT. The MPPT charger tracks the TEG module operating point by controlling its output current such that the TEG module array achieves the maximum output power under the TEG module array configuration. The reconfiguration controller computes the optimal TEG module array configuration according to the instantaneous spatial temperature distribution on the vehicle radiator and controls the ON/OFF states of the switches. The reconfiguration algorithm is periodically executed by the controller and keeps the optimal TEG module array configuration setup at all times.

[1]We call this is the loss: the difference between the power output with MPPT micro-converters and that with a fixed regular array with a single converter.

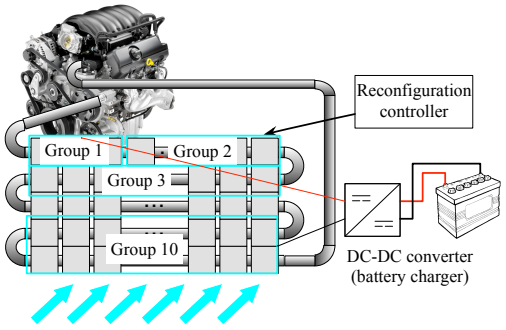

Fig. 6. A system diagram of a reconfigurable TEG heat energy harvesting system from a vehicle radiator.

We provide the formulation of the TEG module array reconfiguration problem in the following:

TEG Module Array Reconfiguration Problem Statement: **Given** TEG module array along the radiator fins with instantaneous spacial temperature variation $T_{pf}[i]$ for $1 \leq i \leq N$, **Find** the optimal TEG module configuration C^{opt} and the TEG module array operating point (V_{array}, I_{array}), **Maximize** the battery charging current I_{batt}.

IV. TEG Module Array Reconfiguration Algorithms

The ultimate goal of the TEG module array reconfiguration is to find the TEG module array configuration $C(g; r_1, r_2, ..., r_g)$ such that each TEG module in the array can work near its MPP. Given the temperature distribution of the radiator and the TEG module array configuration, we estimate the MPP power of the TEG module array based on the MPP voltage and current of each TEG module.

The TEG module groups connected in parallel have the same terminal voltage. Each TEG module is modeled by a series connected current source and a series resistance. The the TEG modules in the same parallelly connected group must have similar ΔT_i and thus similar MPP voltage values to avoid being severely off from their MPP. The MPP voltage of TEG modules in the same group, r_i, should be close with each other. Therefore, we assume that the terminal voltage of r_i is an average MPP voltage of TEG modules in r_i without appreciably sacrificing the fidelity saving a lot of burden for online computation. After we determine the terminal voltage, we find the current of each TEG module in r_i to take the summation of those and derive the current of r_i.

Given a TEG array configuration $C(g; r_1, r_2, ..., r_g)$, we find the configuration such that the summation of the MPP currents in each TEG module group is well balanced (i.e., as close to each other as possible.)

Algorithm 1: TEG Module Array Reconfiguration

Input: The TEG module array temperature profile i.e., $T_{pf}[i]$ for $1 \leq i \leq N$.
Output: The optimal TEG module array configuration i.e., $\boldsymbol{C}^{opt}(r_1^{opt})$.
Calculate the MPP current of each TEG module i.e., I_i^{MPP}, based on $T_{pf}[i]$ for $1 \leq i \leq N$.
$P^{max} = 0$;
for r_1 *from* 1 *to* $N-1$ **do**
  $j = 1$;
  while $\sum_{i=(\sum_{k=1}^{j} r_k)+1}^{N} I_i^{MPP} > \sum_{i=1}^{r_1} I_i^{MPP}$ **do**
    $j = j + 1$;
    Find the value of r_j such that $\sum_{i=(\sum_{k=1}^{j-1} r_k)+1}^{(\sum_{k=1}^{j} r_k)-1} I_i^{MPP} \leq \sum_{i=1}^{r_1} I_i^{MPP} \leq \sum_{i=(\sum_{k=1}^{j-1} r_k)+1}^{\sum_{k=1}^{j} r_k} I_i^{MPP}$.
  end
  Generate three configurations i.e., $C(j+1; r_1, r_2, ..., r_j, N - \sum_{k=1}^{j} r_k)$, $C(j; r_1, r_2, ..., r_{j-1}, N - \sum_{k=1}^{j-1} r_k)$, and $C(j; r_1, r_2, ..., r_j)$.
  Pick the configuration with the highest MPP power as $\boldsymbol{C}(r_1)$.
  if *MPP power of* $\boldsymbol{C}(r_1) \geq P^{max}$ **then**
    P^{max} = MPP power of $\boldsymbol{C}(r_1)$;
    $r_1^{opt} = r_1$;
    $\boldsymbol{C}^{opt}(r_1^{opt}) = \boldsymbol{C}(r_1)$;
  end
end

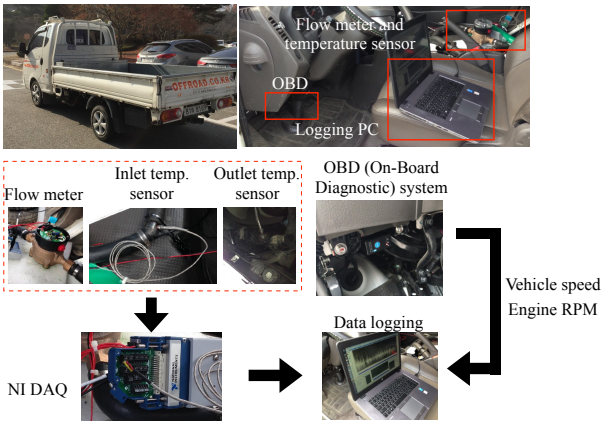

Fig. 7. Vehicle radiator experiment setup using a 3.0L diesel pickup truck.

The reconfiguration algorithm to find $C(g; r_1, r_2, ..., r_g)$ such that i) TEG modules in each group, r_i, have similar ΔT_i, ii) each r_i value is similar among each other and iii) the sum of terminal voltage of r_i is close to 13.8 V. The reconfiguration algorithm has two parts; one is an outer loop that searches the number of TEG modules in r_1, and the other part is a kernel procedure that fixes the TEG module array configuration according to $\boldsymbol{C}(r_1)$. The configuration $\boldsymbol{C}^{opt}(r_1^{opt})$ resulting in the array MPP power is chosen and returned as the optimal configuration under the current TEG module array hot side temperature distribution. The pseudo-code of the reconfiguration algorithm is shown in Algorithm 1.

The kernel procedure receives the number of TEG modules in the first TEG module group, r_1 from the outer loop and determines the number of TEG modules in the second TEG module group, r_2. The summation of the MPP currents of TEG modules in the second group is the closest to the summation of MPP currents of TEG modules in the first group:

$$\sum_{i=r_1+1}^{r_1+r_2-1} I_i^{MPP} \leq \sum_{i=1}^{r_1} I_i^{MPP} \leq \sum_{i=r_1+1}^{r_1+r_2} I_i^{MPP} \qquad (13)$$

where I_i^{MPP} denotes the MPP current of the i-th TEG module. Likewise, we determine r_3, r_4, and so on.

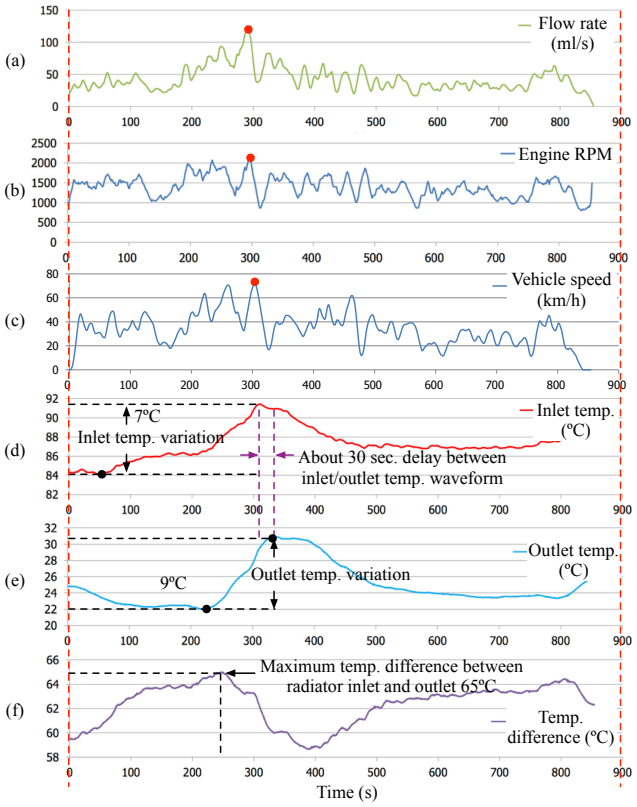

Fig. 8. Measured trace of the radiator coolant flow rate, inlet/outlet temperature and vehicle driving information (engine RPM and vehicle speed.)

We determine the value of r_j and find

$$\sum_{i=r_1+r_2+...+r_j+1}^{N} I_i^{MPP} < \sum_{i=r_1+1}^{r_1+r_2-1} I_i^{MPP}. \qquad (14)$$

The summation of the MPP currents in the rest TEG modules is smaller than the summation of the MPP currents of the TEG modules in the first group. There are three choices for the rest TEG modules such as i) forming the $j+1$-st group, ii) being added to the j-th group, or iii) being bypassed; i) $C(j+1; r_1, r_2, ..., r_j, N - \sum_{k=1}^{j} r_k)$, ii) $C(j; r_1, r_2, ..., r_{j-1}, N - \sum_{k=1}^{j-1} r_k)$, or iii) $C(j; r_1, r_2, ..., r_j)$. We compare the MPP power of the three configurations and pick the one with the highest MPP power as $\boldsymbol{C}(r_1)$ (i.e., the returned result of the kernel procedure.)

V. Experimental Results

A. Vehicle Radiator Experiments

We measure the vehicle coolant flow rate, inlet temperature, outlet temperature, engine RPM, vehicle speed, etc. from a regular cab 3.0 L diesel pickup truck (Hyundai Porter II) with a radiator size of 665 mm × 385 mm as shown in Fig. 7. We use a Recordall industrial flow meter to measure the coolant flow rate. We obtain the coolant inlet and outlet temperature of the radiator using thermocouple probes (model: TC-K-NPT-U-72), which are mounted at the inlet and outlet of the radiator. A National Instrument (NI) data acquisition (DAQ) module is used to log the flow rate and inlet/outlet temperature. We extract driving information such as engine RPM (revolutions per minute) and vehicle speed by accessing the onboard diagnostic (OBD II) system. Fig. 8 shows the measured trace of radiator coolant flow rate, inlet/outlet temperature and vehicle

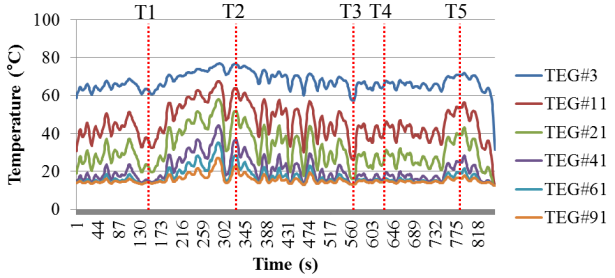

Fig. 9. The extracted temperature distribution trace of the radiator.

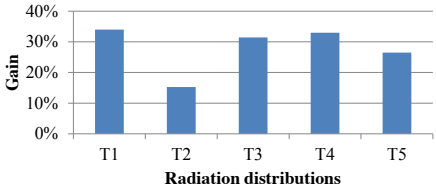

Fig. 10. The performance enhancement by the dynamic reconfiguration.

driving information (engine RPM, vehicle speed) during the a test driving period. The flow rate is highly correlated to the engine RPM because the coolant pump is driven by the serpentine belt. Coolant temperature is related to the engine RPM, vehicle speed and engine temperature, and they show similar patterns and the maximum values (shown in red dots.)

Fig. 8 (d)-(f) shows the transitions in the radiator inlet and outlet temperatures and the difference between while the truck is driven. There is a certain time delay in the coolant temperature values between inlet and outlet of the radiator (around 30 s), which causes a large variations in the spatial temperature difference. The temperature difference between radiator inlet and outlet is up to $65°C$, which really limits the effectiveness of the MPP tracking for a fixed regular TEG module array.

We obtain the temperature distribution inside the radiator based on the radiator model discussed in Section II-A. Radiator pins, heatsinks, are attached to the top ceramic plates of the TEG modules and are exposed to the ambient air convection, which is around $10°C$ in our experiments. The bottom ceramic plates of the TEG modules are attached to the designated locations of on the radiator surface. Fig. 9 shows the extracted temperature distribution trace in the radiator that gradually but significantly decreases.

B. Performance Evaluation

The target radiator can accommodate up to 100 TEG modules which are limited by the surface area of the target radiator. The physical location of the TEG modules is fixed at the system design stage. The proposed TEG system is comprised of a TEG module array, a TEG charger of Linear Technology LTM4607 converter and a vehicle battery with a charging voltage of 13.8 V. We compare the performances of the proposed dynamic reconfiguration of the TEG module array with a baseline, which is a fixed regular 10 by 10 TEG module array. We apply the MPPT proposed in [13]. For the comparison with the state-of-the-art technologies, we also assume bypass diodes with the baseline TEG modules to enhance power output [14].

We use five benchmark temperature distributions (T1 to T5) for performance evaluation of the dynamic reconfiguration from the extracted temperature distribution radiator traces in Fig. 9. Fig. 10 shows the performance enhancement of the dynamic reconfiguration compared with the 10 by 10 fixed TEG module array. We obtain power gain by the dynamic reconfiguration from 15% to 34%. Radiator inlet temperature is rapidly decreased in Benchmarks T1, T3 and T4. Irregular TEG module power by these radiation temperature variation causes power loss in the 10 by 10 fixed TEG module array. Therefore, we obtain larger power gains by the dynamic reconfiguration in these benchmarks.

VI. Conclusion

This paper introduces a novel system-level solution for thermoelectric generator (TEG) modules attached to a vehicle radiator. TEG energy harvesting has been mainly driven by material science and device research groups, and therefore, the proposed dynamic reconfiguration is the first attempt to enhance the power efficiency using a system-level solution while it offers significant performance enhancement at low development cost. Such a system-level solution can be hardly achieved by conventional material and device research. The practical aspects of the proposed research has been strongly backed up by actual vehicle radiator measurement demonstrating up to a 34% performance enhancement compared with common practices.

Acknowledgment

This work was supported by the National Research Foundation of Korea (NRF) Grant funded by the Korean Government (MSIP) (NRF-2015R1A5A1036133.)

References

[1] A. Eder and M. Linde, "Efficient and dynamic–the bmw group roadmap for the application of thermoelectric generators," in *Second Thermoelectric Applications Workshop, San Diego*, 2011.

[2] R. S. Badekar, J. S. Mahajan, S. G. Kakaye, P. N. Khire, and K. Gopalakrishna, "Development of control system for electrical radiator fan using dual sensor & microprocessor based electronic unit," tech. rep., SAE Technical Paper, 2006.

[3] T. T. Wang, A. Jagarwal, J. R. Wagner, and G. Fadel, "Optimization of an automotive radiator fan array operation to reduce power consumption," *IEEE/ASME Transactions on Mechatronics*, vol. 20, no. 5, pp. 2359–2369, 2015.

[4] L. Garg and R. Singh, "Reverse engineering and design optimization of radiator fan maruti-800," *International Journal of Engineering Science*, vol. 4179, 2016.

[5] T. L. Bergman and F. P. Incropera, *Introduction to heat transfer*. John Wiley & Sons, 2011.

[6] Y. Wang, C. Dai, and S. Wang, "Theoretical analysis of a thermoelectric generator using exhaust gas of vehicles as heat source," *Applied Energy*, vol. 112, pp. 1171–1180, 2013.

[7] S. Kim, S. Park, S. Kim, and S.-H. Rhi, "A thermoelectric generator using engine coolant for light-duty internal combustion engine-powered vehicles," *Journal of electronic materials*, vol. 40, no. 5, pp. 812–816, 2011.

[8] J. Vazquez, M. Sanz-Bobi, R. Palacios, and A. Arenas, "State of the art of thermoelectric generators based on heat recovered from the exhaust gases of automobiles," in *7th European Workshop on Thermoelectric, Proceedings of*, 2002.

[9] C. Goupil, W. Seifert, K. Zabrocki, E. Mller, and G. J. Snyder, "Thermodynamics of thermoelectric phenomena and applications," *Entropy*, vol. 13, no. 8, pp. 1481–1517, 2011.

[10] H. Nagayoshi, K. Tokumisu, and T. Kajikawa, "Novel maximum power point tracking control system for thermoelectric generator and evaluation of mismatch power loss reduction," in *The 5th European Conference on Thermoelectrics, Odessa House of Scientists, Odessa, Ukraine*, 2007.

[11] X. Lin, Y. Wang, S. Yue, D. Shin, N. Chang, and M. Pedram, "Near-optimal, dynamic module reconfiguration in a photovoltaic system to combat partial shading effects," in *Proceedings of the 49th Annual Design Automation Conference*, pp. 516–521, ACM, 2012.

[12] S. Carreon-Bautista, A. Eladawy, A. N. Mohieldin, and E. Snchez-Sinencio, "Boost converter with dynamic input impedance matching for energy harvesting with multi-array thermoelectric generators," *IEEE Transactions on Industrial Electronics*, vol. 61, pp. 5345–5353, Oct 2014.

[13] N. Femia, G. Petrone, G. Spagnuolo, and M. Vitelli, "Optimization of perturb and observe maximum power point tracking method," *IEEE transactions on power electronics*, vol. 20, no. 4, pp. 963–973, 2005.

[14] H. M. Hiroshi Nagayoshi, Kenta Tokumitsu and T. Kajikawa, "High efficiency maximum power point tracking power conditioner for teg systems," in *ECT 2008-6th European Conference on Thermoelectrics*, 2008.